Journal of Sound and Vibration (2002) **255**(3), 457–479
doi:10.1006/jsvi.2001.4165, available online at http://www.idealibrary.com on IDEAL®

H-ADAPTIVE REFINEMENT STRATEGY FOR ACOUSTIC PROBLEMS WITH A SET OF NATURAL FREQUENCIES

F. J. Fuenmayor, F. D. Denia, J. Albelda and E. Giner

Departamento de Ingeniería Mecánica y de Materiales, Universidad Politécnica de Valencia, Camino de Vera s/n, 46022 *Valencia, Spain. E-mail: ffuenmay@mcm.upv.es*

(*Received* 19 *July* 2001, *and in final form* 15 *October* 2001)

The finite element method has been applied to the analysis of acoustic problems with several natural frequencies and mode shapes. First, a recovery-based error estimation is performed following the well-known procedures of structural problems. Then, an *h*-adaptive refinement strategy is proposed that leads to a finite element mesh with the minimum number of elements and with a specified error for each of the natural frequencies included in the analysis. The procedure provides a useful numerical tool, since the computational requirements are reduced. In addition, results obtained by means of the minimum element size procedure are shown for comparison purposes. The similarity of the meshes given by the two methods is justified on the basis of the equations that lead to the element size of the mesh. The procedure has been applied to some numerical examples to illustrate its validity.

1. INTRODUCTION

Acoustic problems are usually modelled by means of analytical and numerical techniques. While the former have important computational advantages when the domains and the boundary conditions are relatively simple (see reference [1] for elliptical domains and reference [2] for the circular case), the latter are useful for arbitrary geometries, at the cost of higher computational requirements. In this case, it is important to define numerical procedures so that the final mesh leads to the prescribed accuracy with a minimum computational cost. Since the acoustic response of a system is usually affected by several of its natural frequencies and mode shapes, a method that enables one to obtain a single mesh with a minimum number of degrees of freedom and a specified error for each natural frequency appears to be a desirable tool for the numerical modelling of acoustic problems. The basic structure of the method can be divided into: (1) estimation of the discretization error; (2) development of the strategy associated with the *h*-adaptive refinement; and (3) mesh generation. While the present work deals with the first and second parts of the previous structure, details of mesh generation procedures can be found elsewhere [3].

Some procedures to estimate the discretization error for acoustic problems with harmonic excitation can be found in the literature. Bouillard *et al.* [4] adapted the superconvergent patch recovery technique (SPR) proposed by Zienkiewicz and Zhu [5, 6] to acoustic problems, considering complex variables. This work showed that the error estimator depends on the frequency of excitation. Ihlenburg and Babuška [7, 8] studied the finite element error of the solution of the Helmholtz equation when a high wave number is considered. They showed that the total error can be divided into two terms: a local error which can be estimated with the traditional recovery techniques that perform local

0022-460X/02/$35.00

calculations, and a global error related to the pollution of the solution, which is associated with a phase lag between the exact and the numerical solution. This pollution term can be neglected in the asymptotic range, that is, when the mesh is very refined, but it becomes important in the preasymptotic range [9], in which the standard *a posteriori* estimates based only on local computations underestimate the exact error. For the kind of meshes and frequency range considered in the present work, the pollution error has not been taken into account.

In the case of natural frequencies and mode shapes, most of the reported works that deal with error estimation are applied to structural problems, showing that the patch recovery techniques usually lead to good results. In references [10, 11], the SPR technique was used to improve the stress field associated with each natural mode and to estimate the error of the corresponding natural frequency. Stephen and Steven [12] considered the displacement modal field given by finite element calculations in a patch in order to improve it via a weighted least-squares technique. This enabled them to evaluate more accurate eigenvalues, which were used as an error measure for the original finite element analysis. Hager and Wiberg [13] proposed a modification of the SPR technique, based on the displacement field (SPRD) rather than the stress field. The improved displacement field led to a better estimation of the natural frequencies. The results were shown to be quite good, mainly for regular meshes and low order mode shapes. The present work applies the SPR technique adapted to acoustics [4] in order to estimate the discretization error in acoustic eigenfrequencies. This means that the acoustic pressure gradient associated with each mode shape is improved in order to be compared with the original finite element solution, enabling one to obtain an error estimation of the acoustic natural frequencies. As will be shown from numerical examples, the error estimation is found to be acceptable for engineering purposes, that is, the effectivity index is close to unity as the mesh is refined.

Once the discretization error has been estimated, the desired error can be achieved by remeshing the original finite element mesh based on the error estimation. Some reported works that deal with *h*-adaptivity in acoustics consider the problem of frequency response for a single frequency of excitation. In references [14, 15], the SPRD technique was applied to obtain a better pressure field. This leads to the optimum mesh for a given frequency of excitation by considering the criterion of achieving equal error in each element of the new mesh. As far as the eigenproblem is concerned, the reported papers dealing with *h*-adaptive refinement mainly consider structural problems. Hager and Wiberg [13] considered the optimum mesh for a single natural frequency. The works of Ladeveze *et al.* [16] and Ladeveze and Pelle [17] studied the performance of the optimum mesh for a set of natural frequencies, defining as the optimum mesh the one that achieves a mean error in the set of eigenvalues lower than the desired error, with a minimum number of elements. References [10, 11] defined *h*-adaptive strategies in order to obtain the optimum mesh for a set of natural frequencies, considering, in a general way, a desired error which can be different for each mode shape.

The strategy developed in this work is applied to two bidimensional test problems. First, a problem with exact analytical solution is considered (a rectangular cavity), which enables one to validate the procedure. Secondly, a more complex geometry similar to the one considered in reference [14] is analyzed.

2. ACOUSTIC NATURAL FREQUENCIES AND MODE SHAPES

The propagation of sound in an ideal fluid is governed by the well-known wave equation [18]

$$\Delta p_a = \frac{1}{c_0^2} \frac{\partial^2 p_a}{\partial t^2}, \tag{1}$$

Δ being the Laplacian operator, p_a the acoustic pressure, c_0 the speed of sound and t the time variable. If the finite element formulation is applied to equation (1), the problem of natural frequencies and mode shapes can be expressed, under harmonic behavior, as

$$([\mathbf{K}] - \omega^2[\mathbf{M}])\{\mathbf{P}_a\} = \{\mathbf{0}\}, \tag{2}$$

where $[\mathbf{K}]$ is defined as the "classical" stiffness matrix, related to the acoustic kinetic energy, $[\mathbf{M}]$ the "classical" mass matrix, associated with the acoustic potential energy, ω the angular frequency and $\{\mathbf{P}_a\}$ the vector containing the nodal values of the pressure amplitude field. The matrices $[\mathbf{K}]$ and $[\mathbf{M}]$ are both real and symmetric. The solution of this eigenproblem is a set of natural frequencies $\omega_{fe(r)}$ and mode shapes $\{\mathbf{P}_a\}_{fe(r)}$, where r denotes the mode number.

If one considers the modal transformation of co-ordinates, the modal mass $m_{fe(r)}$ and the modal stiffness $k_{fe(r)}$ can be defined as

$$\{\mathbf{P}_a\}^{\mathrm{T}}_{fe(r)}[\mathbf{K}]\{\mathbf{P}_a\}_{fe(r)} = k_{fe(r)}, \tag{3}$$

$$\{\mathbf{P}_a\}^{\mathrm{T}}_{fe(r)}[\mathbf{M}]\{\mathbf{P}_a\}_{fe(r)} = m_{fe(r)}, \tag{4}$$

where the natural frequency is given by

$$\omega^2_{fe(r)} = \frac{k_{fe(r)}}{m_{fe(r)}}. \tag{5}$$

Introducing the errors in modal stiffness $\Delta k_{(r)} = k_{fe(r)} - k_{ex(r)}$ and modal mass $\Delta m_{(r)} = m_{fe(r)} - m_{ex(r)}$ ($m_{ex(r)}$ and $k_{ex(r)}$ denoting exact values) as the difference between the finite element and the exact solution, the exact natural frequencies $\omega_{ex(r)}$ can be expressed in terms of their associated modal mass and stiffness. Therefore, the following relationship holds:

$$\omega^2_{ex(r)} = \frac{k_{ex(r)}}{m_{ex(r)}} = \frac{k_{fe(r)} - \Delta k_{(r)}}{m_{fe(r)} - \Delta m_{(r)}}. \tag{6}$$

If the mode shapes are supposed to be normalized so that $m_{fe(r)} = m_{ex(r)} = 1$, the combination of equations (5) and (6) leads to the error in natural frequency $e_{\omega ex(r)}$, given by

$$e^2_{\omega ex(r)} = \omega^2_{fe(r)} - \omega^2_{ex(r)} = k_{fe(r)} - k_{ex(r)} = \Delta k_{(r)}. \tag{7}$$

The normalization of the mode shapes enables one to define the error in natural frequency as a function of the error in modal stiffness. When consistent mass matrices are considered, the discretization error arises mainly from the kinetic energy modelling [11]. Since only consistent mass matrices are included in the present work, the normalization is found to be suitable.

3. ESTIMATION OF THE DISCRETIZATION ERROR

The evaluation of the discretization error can be approached by considering the norm of the exact acoustic pressure field p_{aex}

$$\| p_{aex} \| = \left[\int_V (\nabla p_{aex})^{\mathrm{T}} \nabla \tilde{p}_{aex} \mathrm{d}V \right]^{1/2}, \tag{8}$$

where ∇ is the gradient operator, the symbol "$\sim$" denotes the complex conjugate and V the volume of the fluid domain. The squared norm of the finite element solution $p_{afe(r)}$ is related to the kinetic energy, and is given by

$$\| p_{afe(r)} \|^2 = \int_V (\nabla p_{afe(r)})^{\mathrm{T}} \nabla \tilde{p}_{afe(r)} \, \mathrm{d}V = \{\mathbf{P}_a\}^T_{fe(r)} [\mathbf{K}] \{\mathbf{P}_a\}_{fe(r)} = k_{fe(r)}. \tag{9}$$

For problems in which no Dirichlet boundary conditions exist, one has $\| p_{aef(1)} \| = 0$ since $p_{aef(1)}$ is constant. If equation (8) is required to be a norm for all practical considerations, only higher order modes ($r > 1$) have to be included in the analysis. The squared norm of the exact discretization error $e_{ex(r)}$ is given by

$$\| e_{ex(r)} \|^2 = \| p_{aex(r)} - p_{afe(r)} \|^2 = \int_V (\nabla p_{aex(r)} - \nabla p_{afe(r)})^{\mathrm{T}} (\nabla \tilde{p}_{aex(r)} - \nabla \tilde{p}_{afe(r)}) \, \mathrm{d}V. \tag{10}$$

The consideration of consistent mass matrices and appropriate conditions related to the numerical integration [19], lead to the following convergence relation:

$$0 \leqslant e^2_{\omega ex(r)} = \omega^2_{fe(r)} - \omega^2_{ex(r)} \leqslant C h^{2p}, \tag{11}$$

h being the element size, p the polynomial degree of the pressure interpolation functions and C a positive constant which depends on p and the mode considered, but not on h. The error in norm, defined as the difference between the norm of the exact solution and that of the finite element solution, is not completely equivalent to the norm of the error. From equations (7), (9) and (11), and applying the triangular inequality, the error in natural frequency $e^2_{\omega ex(r)}$ satisfies the following relationship,

$$\begin{aligned} e^2_{\omega ex(r)} &= \| p_{afe(r)} \|^2 - \| p_{aex(r)} \|^2 = \| p_{afe(r)} - p_{aex(r)} + p_{aex(r)} \|^2 - \| p_{aex(r)} \|^2 \\ &\leqslant \| p_{afe(r)} - p_{aex(r)} \|^2 + \| p_{aex(r)} \|^2 - \| p_{aex(r)} \|^2 = \| p_{aex(r)} - p_{afe(r)} \|^2 \\ &= \| e_{ex(r)} \|^2. \end{aligned} \tag{12}$$

For practical purposes, the inequality expressed in equation (12) is replaced by the approximation "$\approx$" in order to obtain the formulation that leads to the h-adaptive refinement, which can be accepted in the asymptotic range of convergence. To estimate the absolute discretization error, a recovered pressure gradient field ∇p^*_a is used in equation (10) (see reference [4]) instead of the exact one, which is generally unknown. This leads to

$$e^2_{\omega es(r)} \approx \| e_{es(r)} \|^2 = \int_V (\nabla p^*_{a(r)} - \nabla p_{afe(r)})^{\mathrm{T}} (\nabla \tilde{p}^*_{a(r)} - \nabla \tilde{p}_{afe(r)}) \, \mathrm{d}V, \tag{13}$$

the subscript *es* denoting estimated variables. The behavior of the error estimator depends strongly on the procedure applied to obtain the recovered pressure gradient field. The method of direct nodal averaging for linear triangular elements and the SPR technique [4] for quadratic triangular elements are considered here. The relative exact error $\eta_{ex(r)}$ is defined as

$$\eta_{ex(r)} = \frac{\| e_{ex(r)} \|}{\| p_{aex(r)} \|}. \tag{14}$$

In order to estimate $\|p_{aex(r)}\|$, one may use the expression $\|p_{afe(r)}\|^2 - \|p_{aes(r)}\|^2 \approx \|e_{es(r)}\|^2$ based on equation (12) with estimated values. Finally, the estimated relative error can be defined as

$$\eta_{es(r)} = \frac{\|e_{es(r)}\|}{\sqrt{\|p_{aef(r)}\|^2 - \|e_{es(r)}\|^2}}. \tag{15}$$

4. H-ADAPTIVE STRATEGY

An *h*-adaptive strategy is proposed considering an optimum mesh that enables one to obtain a specified error with a minimum number of elements [20–22], since this strategy has been shown to be suitable for problems with several load cases. The criterion of minimizing the number of elements has been found to give similar results to the technique associated with the uniform absolute error distribution procedure [23, 24].

The element size in the new mesh can be defined considering the local refinement ratio $R_{(r)}^{(e)}$ for each mode shape

$$R_{(r)}^{(e)} = \frac{h_{pre(r)}^{(e)}}{h_{new(r)}^{(e)pre}}, \tag{16}$$

with $h_{new(r)}^{(e)pre}$ being the element size in the new mesh of those elements contained in the element e of the previous mesh whose size is $h_{pre(r)}^{(e)}$. The number of elements $N_{new(r)}^{(e)pre}$ with size $h_{new(r)}^{(e)pre}$ can be approximated by means of

$$N_{new(r)}^{(e)pre} \approx (R_{(r)}^{(e)})^D, \tag{17}$$

with D being the dimension of the problem. Here, only bidimensional geometries are taken into account ($D = 2$), and therefore the new mesh has a total number of elements $N_{new(r)}$ given by

$$N_{new(r)} \approx \sum_{e=1}^{N_{pre(r)}} (R_{(r)}^{(e)})^2, \tag{18}$$

where $N_{pre(r)}$ is the number of elements of the previous mesh. If the domain associated with element e of the previous mesh is considered, it is possible to establish a local convergence relationship similar to that expressed in equation (11) in the asymptotic range. Thus, for practical purposes and with estimated values, the discretization errors of two consecutive meshes and the local refinement ratio are related by

$$\frac{e_{\omega es(r)}^{(e)}|_{pre}}{e_{\omega es(r)}^{(e)pre}|_{new}} \approx \left[\frac{h_{pre(r)}^{(e)}}{h_{new(r)}^{(e)pre}}\right]^p = (R_{(r)}^{(e)})^p \tag{19}$$

with $e_{\omega es(r)}^{(e)pre}|_{new}$ being the estimated error for all the elements of the new mesh contained in the element e of the previous mesh whose error is denoted by $e_{\omega es(r)}^{(e)}|_{pre}$. Combining the previous results, an expression is derived that yields the error in the new mesh as a function of the error in the previous mesh and the local refinement ratio,

$$e_{\omega es(r)}|_{new}^2 = \sum_{e=1}^{N_{new(r)}} e_{\omega es(r)}^{(e)}|_{new}^2 = \sum_{e=1}^{N_{pre(r)}} e_{\omega es(r)}^{(e)pre}|_{new}^2 \approx \sum_{e=1}^{N_{pre(r)}} (e_{\omega es(r)}^{(e)}|_{pre}^2 (R_{(r)}^{(e)})^{-2p}). \tag{20}$$

4.1. OPTIMUM MESH FOR A SINGLE MODE SHAPE

Following the previous results, the optimum mesh for a mode shape can be achieved by finding the local refinement ratio that minimizes

$$N_{new(r)} = \sum_{e=1}^{N_{pre(r)}} (R_{(r)}^{(e)})^2, \tag{21}$$

constrained to

$$\sum_{e=1}^{N_{pre(r)}} (e_{\omega es(r)}^{(e)}|_{pre}^2 (R_{(r)}^{(e)})^{-2p}) - e_{\omega(r)}|_d^2 = 0, \tag{22}$$

where $e_{\omega(r)}|_d$ is the absolute error specified for the mode shape r in the new mesh. The local refinement ratio that satisfies this problem is given by [11, 25]

$$(R_{(r)}^{(e)})^{2(p+1)} = \left[\frac{\sum_{e=1}^{N_{pre(r)}} e_{\omega es(r)}^{(e)} \Big|_{pre}^{\frac{2}{p+1}}}{e_{\omega(r)}|_d^2} \right]^{(p+1)/p} e_{\omega es(r)}^{(e)}|_{pre}^2, \tag{23}$$

which depends on the estimated errors in the previous mesh, and can be evaluated separately for all the modes included in the analysis.

4.2. OPTIMUM MESH FOR A SET OF MODE SHAPES

If N_M modes are included in the analysis simultaneously, the local refinement ratio $R^{(e)}$ for all the modes comes from the solution of the problem associated with minimizing

$$N_{new} = \sum_{e=1}^{N_{pre}} (R^{(e)2}, \tag{24}$$

constrained to

$$\sum_{e=1}^{N_{pre}} (e_{\omega es(r)}^{(e)}|_{pre}^2 (R^{(e)})^{-2p}) - e_{\omega(r)}|_d^2 = 0, \quad r = 1, \ldots, N_M. \tag{25}$$

The solution of the previous problem [11, 25] shows that the local refinement ratio for a set of modes depends on the local refinement ratio of each mode, that is,

$$(R^{(e)})^{2(p+1)} = \sum_{r=1}^{N_M} [\xi_{(r)} (R_{(r)}^{(e)})^{2(p+1)}] \tag{26}$$

with $\xi_{(r)}$ being the global refinement contribution factor of the mode r, that satisfies the following set of equations:

$$\sum_{e=1}^{N_{pre}} \left[e_{\omega es(r)}^{(e)}|_{pre}^2 \left(\sum_{j=1}^{N_M} \xi_{(j)} (R_{(j)}^{(e)})^{2(p+1)} \right)^{-p/(p+1)} \right] = e_{\omega(r)}|_d^2, \quad r = 1, \ldots, N_M. \tag{27}$$

The refinement associated with some modes, however, can suitably refine the mesh for other modes, as it is shown qualitatively in Figure 1, in which the relative error of two particular

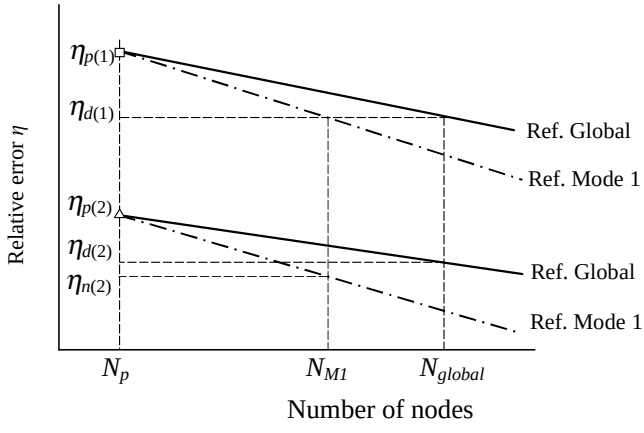

Figure 1. Relative error of two modes versus number of nodes for different refinement processes.

modes is represented as a function of the number of nodes of the finite element mesh. The previous mesh has N_p nodes, and the relative errors in each mode are $\eta_{p(1)}$ and $\eta_{p(2)}$ respectively. The new mesh is required to give desired relative errors $\eta_{d(1)}$ and $\eta_{d(2)}$. If only the first mode is included in the refinement process, the errors follow the line 'Ref. Mode 1', and N_{M1} nodes are necessary to achieve a value less than or equal to the desired error for the first mode. In this case, the error for the second mode in the new mesh, $\eta_{n(2)}$, is found to be less than the desired one, that is, $\eta_{n(2)} < \eta_{d(2)}$. However, if both modes are taken into account in the refinement (line 'Ref. Global'), the error will be equal to the desired one for both of them, at the expense of modifying the mesh as the second mode indicates. This finally leads to a greater number of nodes N_{global}, so that $N_{global} > N_{M1}$. In this case, the global refinement contribution factor $\xi_{(2)}$ is negative. Thus, in order to obtain the optimum mesh with a minimum number of elements, only the first mode should be kept in the refinement. Therefore, the initial problem should be reformulated by means of replacing the equal restriction by a "less than or equal to" constraint in equation (25). The problem can now be stated as minimizing

$$N_{new} = \sum_{e=1}^{N_{pre}} (R^{(e)})^2, \tag{28}$$

constrained to

$$\sum_{e=1}^{N_{pre}} (e^{(e)}_{\omega es(r)}|^2_{pre} (R^{(e)})^{-2p}) - e_{\omega(r)}|^2_d \leqslant 0, \quad r = 1, \ldots, N_M. \tag{29}$$

The optimum mesh could be obtained via the solution of this new problem. Another possibility is to consider equations (24) and (25) and to exclude those modes whose global refinement contribution factor is found to be negative.

4.3. MINIMUM ELEMENT SIZE CRITERION

A practical criterion to define the mesh refinement when dealing with a set of natural frequencies consists of evaluating the local refinement ratio for each mode separately, and

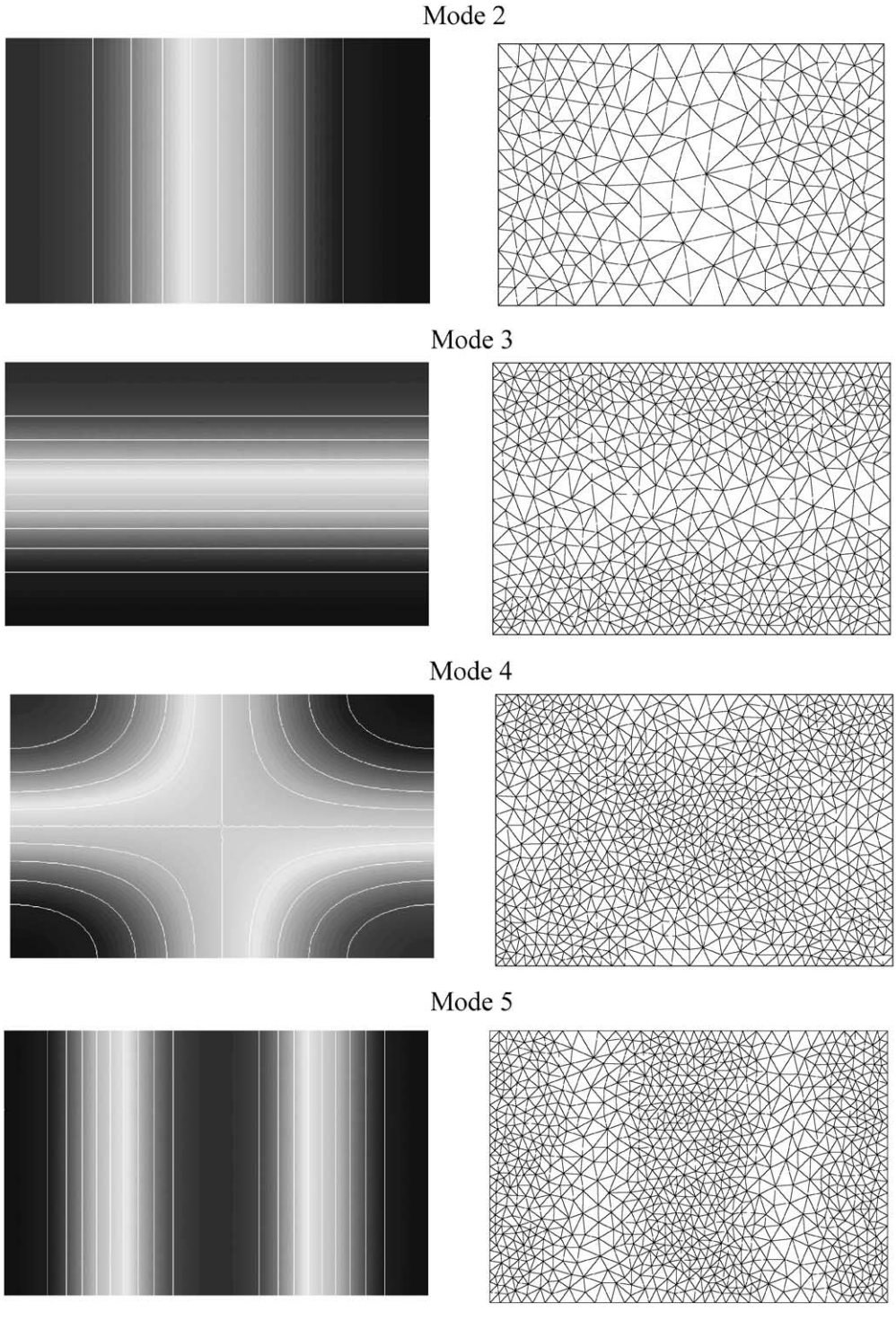

Figure 2. Acoustic mode shapes and optimum finite element meshes of a rectangular cavity (modes considered separately).

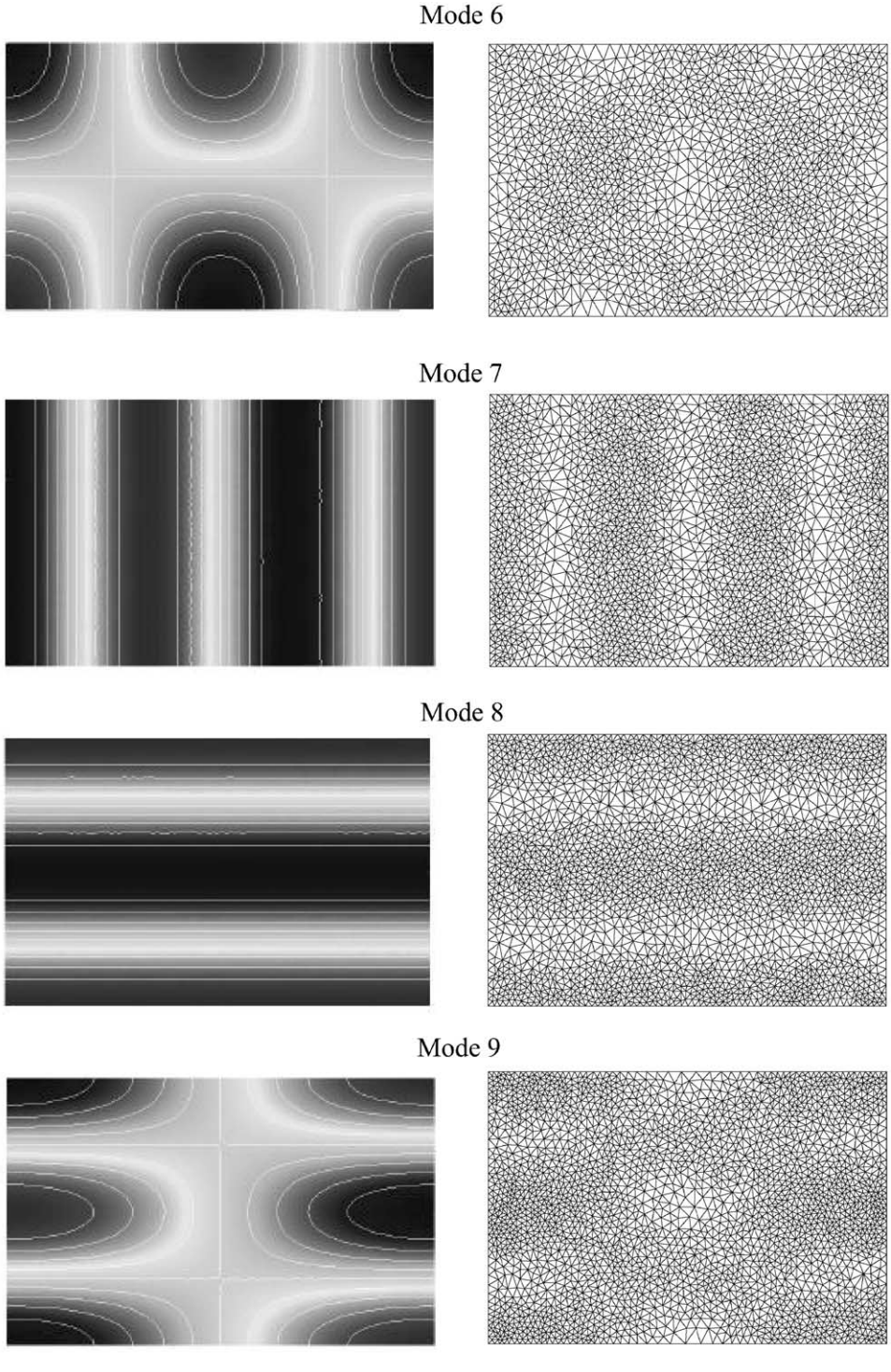

Figure 2. Continued.

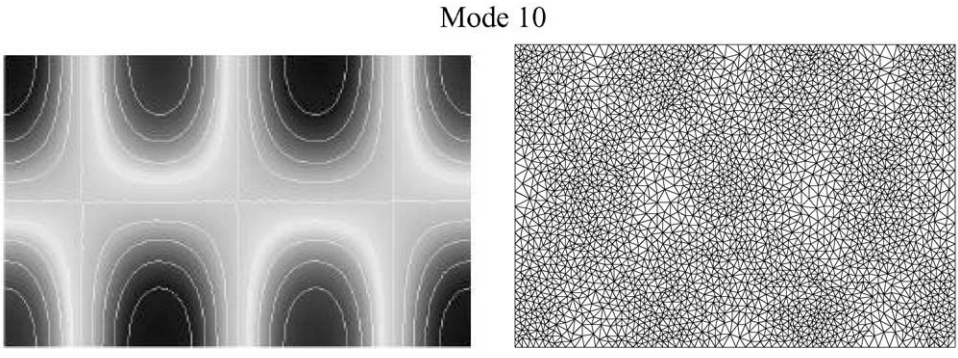

Figure 2. Continued.

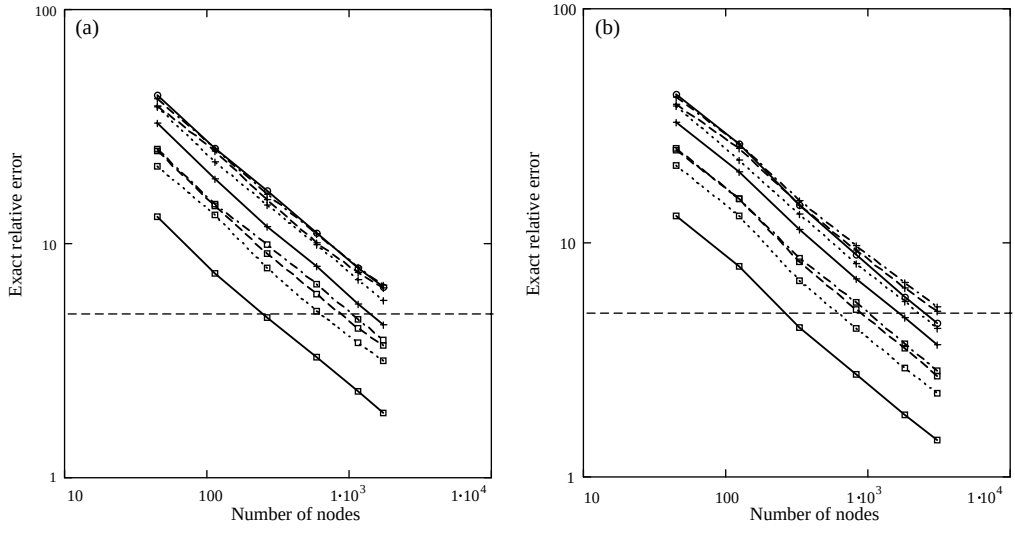

Figure 3. Convergence of the exact relative error: □——□, mode 2; □---□, mode 3; □– – –□, mode 4; □– – – – –□, mode 5; +——+, mode 6; +---+, mode 7; +– – –+, mode 8; +– – – – –+, mode 9; ○——○, mode 10. Mesh obtained considering only (a) mode 6 and (b) mode 10.

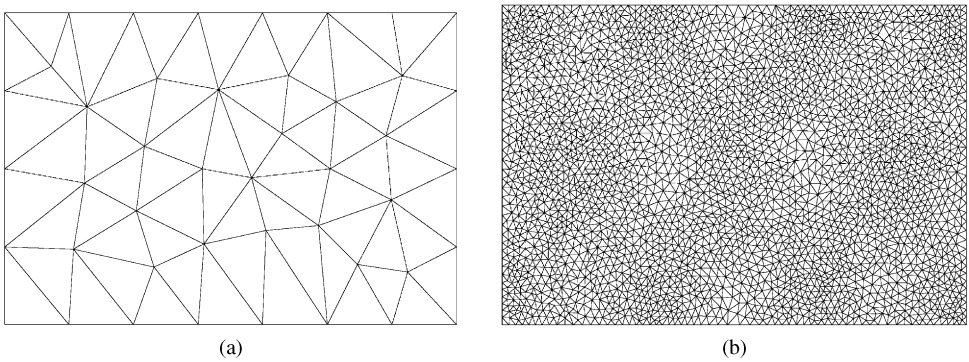

Figure 4. Finite element mesh for a rectangular cavity with all the modes considered simultaneously: (a) starting mesh and (b) final mesh.

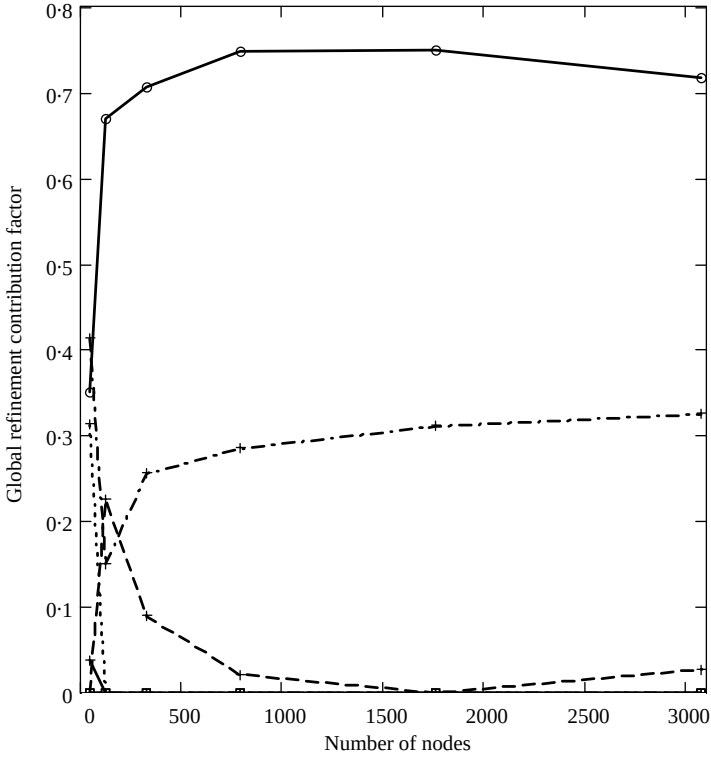

Figure 5. Global refinement contribution factors (legend same as in Figure 3).

then the maximum value is taken, that is

$$R_{min}^{(e)} = \max(R_{(r)}^{(e)}) \tag{30}$$

with $R_{min}^{(e)}$ being the local refinement ratio of the minimum element size criterion. The sequence of meshes provided by this method is quite often very similar to that obtained via the criterion of minimizing the number of elements explained in the previous section. The reason can be found if equation (26) is analyzed. The local refinement ratio $R^{(e)}$ is related to the local refinement ratios of the modes, $R_{(r)}^{(e)}$, which are weighted by the global refinement contribution factors $\xi_{(r)}$. However, the exponent of the local refinement ratio is high (its value is 4 for linear elements and 6 for quadratic elements). This means that the most important contribution to the definition of $R^{(e)}$ comes from the maximum value of $R_{(r)}^{(e)}$. It is obvious that this simple interpretation cannot be valid for all the problems, but the numerical results obtained in several test problems indicate that the differences between both procedures, minimum number of elements and minimum element size, are small from a practical point of view. However, it is important to take into account some remarkable details when the minimum element size criterion is applied. The error obtained with this procedure can be less than the desired one for each mode, due to the fact that some elements are excessively refined. To avoid this situation, it is possible to introduce a scale factor $\beta_{(r)}$ for each mode, so that the refinement is performed by means of $\beta R_{min}^{(e)}$, rather than the term given directly by equation (30). This scale factor β for all the modes considered simultaneously is obtained from

$$\beta = \max(\beta_{(r)}), \tag{31}$$

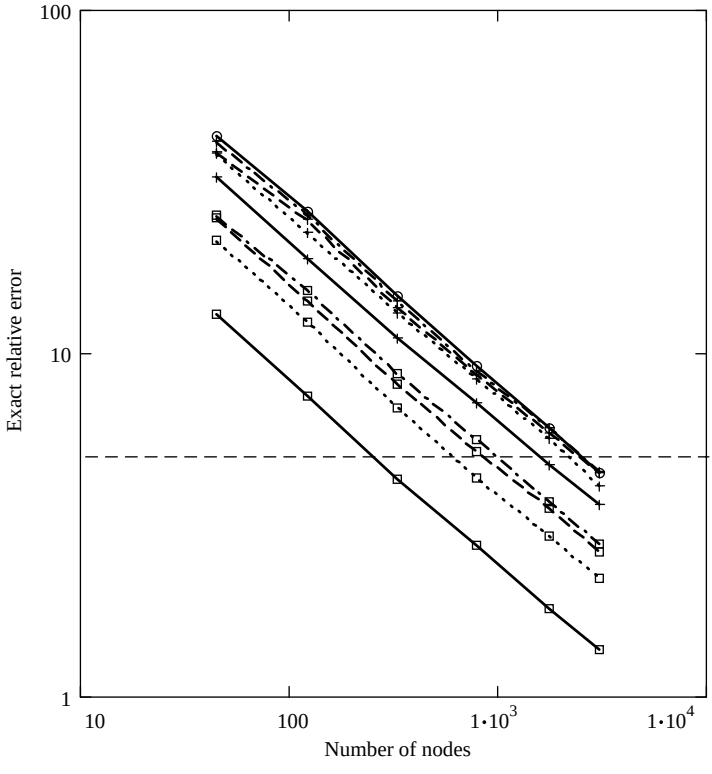

Figure 6. Convergence of the exact relative error with the developed procedure and linear triangular elements (legend same as in Figure 3).

which leads to an error less than or equal to that required in the analysis for each mode. To evaluate the scale factor $\beta_{(r)}$ for each mode, equation (22) turns into

$$\sum_{e=1}^{N_{pre(r)}} (e^{(e)}_{\omega es(r)}|^2_{pre}(\beta_{(r)} R^{(e)}_{min})^{-2p}) - e_{\omega(r)}|^2_d = 0, \tag{32}$$

and $\beta_{(r)}$ is found to be

$$\beta^{-2p}_{(r)} = \frac{e_{\omega(r)}|^2_d}{\sum_{e=1}^{N_{pre(r)}} (e^{(e)}_{\omega es(r)}|^2_{pre}(R^{(e)}_{min})^{-2p})}. \tag{33}$$

Some test problems are shown in the next section, in order to validate the *h*-adaptive refinement strategy proposed in this work, as well as all the aforementioned comments about the minimum element size criterion.

5. RESULTS AND DISCUSSION

Two bidimensional test examples are considered in this section to validate the proposed adaptive strategy and to illustrate its application. The first example consists of a rectangular

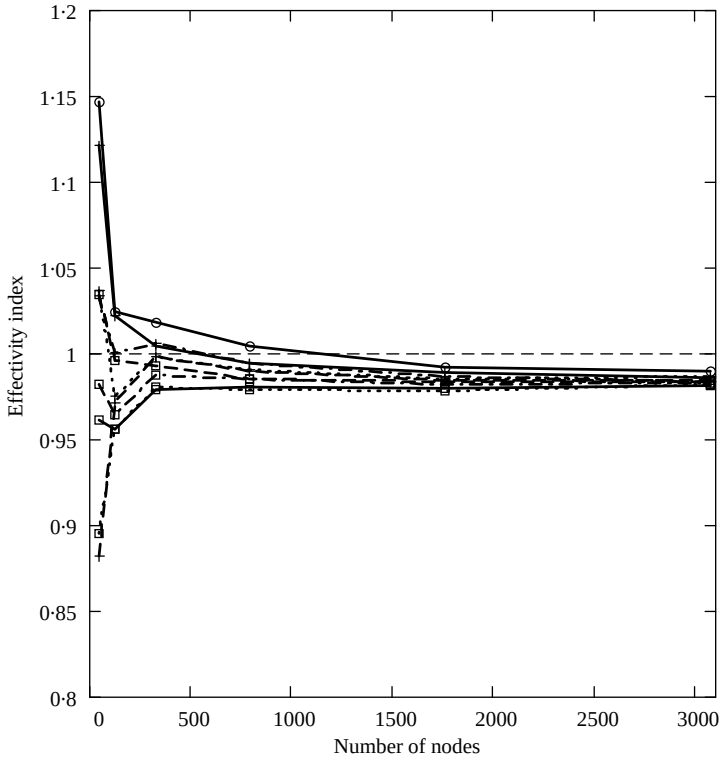

Figure 7. Effectivity index with the developed procedure and linear triangular elements (legend same as in Figure 3).

cavity with closed walls, whose analytical solution is known and enables one to validate the procedure. The rectangle is 1·6 m in length and 1 m in height, the speed of sound is $c_0 = 342{\cdot}57$ m/s and the fluid density $\rho_0 = 1{\cdot}21$ kg/m^3. The analysis includes the mode shapes 2, 3, …, 10 (the mode 1 is not considered since it consists of a uniform pressure field). First, the modes are considered separately, and the optimum mesh has been obtained for each of them. The desired relative error is set to 5 per cent for each mode, and six *h*-adaptive steps are performed to obtain the convergence curve (the starting mesh is the same for all the modes). Figure 2 shows the results obtained (mode shape pressure field and optimum mesh) with linear triangular elements for the aforementioned nine mode shapes arranged according to increasing natural frequency. As can be seen, the element size depends on the solution of the problem, and obviously, it is different for each mode shape.

The optimum refinement achieved for each mode is not able to obtain the desired error for some of the other mode shapes. For instance, the exact relative error,

$$\eta_{ex(r)} = \frac{\sqrt{\omega_{fe(r)}^2 - \omega_{ex(r)}^2}}{\omega_{ex(r)}}, \tag{34}$$

versus the number of nodes of the mesh is depicted in Figure 3, considering the results obtained for modes 6 and 10. If only mode 6 is included in the refinement, the discretization error is less than or equal to the desired one for this mode and those with lower order, but

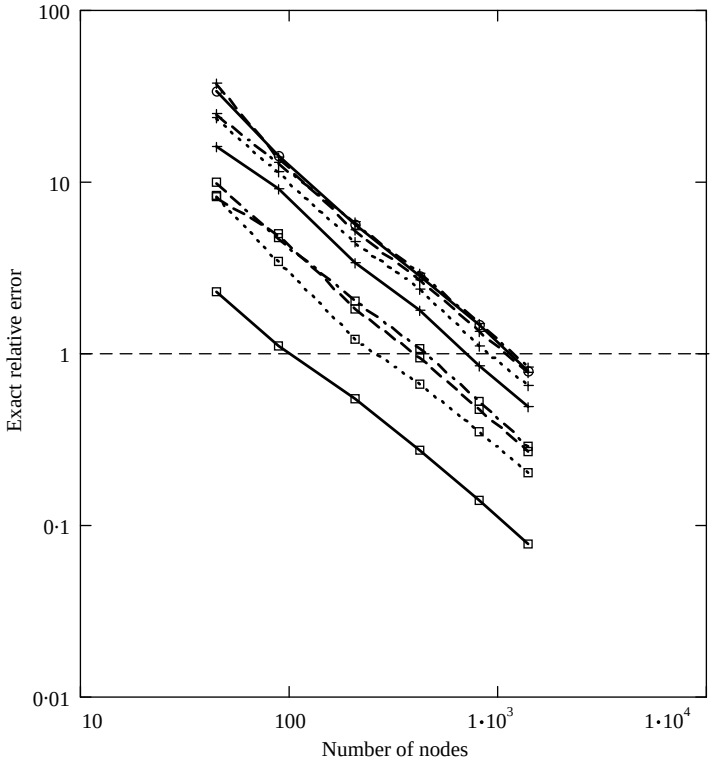

Figure 8. Convergence of the exact relative error with the developed procedure and quadratic triangular elements (legend same as in Figure 3).

the desired error is not achieved for higher order modes. In addition, the highest mode cannot suitably refine some lower order modes, since the mesh obtained considering the mode 10 gives errors higher than the desired one for modes 8 and 9.

The application of the developed procedure allows one to consider all the modes simultaneously. The starting mesh is shown in Figure 4(a), which is equal to that considered in Figure 2. The *h*-adaptive strategy leads to the mesh shown in Figure 4(b), which provides a discretization error less than or equal to the desired one for each mode shape. Figure 5 shows the global refinement contribution factors $\xi_{(r)}$ obtained with the proposed method. The modes that have significant participation are the tenth, ninth and eighth. The rest are sufficiently refined by these modes, and hence, their contribution to the final mesh is negligible. Figure 6 shows the convergence curve of the relative error, which is shown to be less than or equal to than the desired one for each mode.

In order to validate the suitability of the error estimation, the ratio of the estimated error to the exact one can be found, that is,

$$\theta_{(r)} = \frac{\|\mathbf{e}_{es(r)}\|}{\sqrt{\omega^2_{fe(r)} - \omega^2_{ex(r)}}}, \tag{35}$$

where $\theta_{(r)}$ is the effectivity index. This is represented in Figure 7, in which, as can be observed, the effectivity index is close to unity when the number of nodes is increased (the

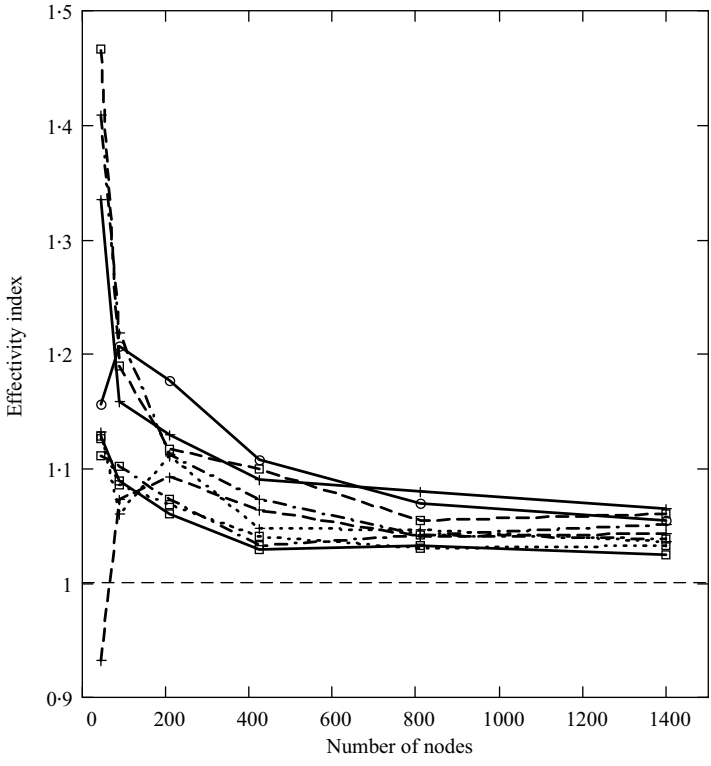

Figure 9. Effectivity index with the developed procedure and quadratic triangular elements (legend same as in Figure 3).

difference can be assessed in relation to truncation errors and tolerances in the evaluation of the eigenvalues, among others). This is in agreement with the fact that the discretization error arises basically from the acoustic kinetic energy term, and that the error associated with the acoustic potential energy can be neglected in practical problems.

The same problem has been solved by means of quadratic triangular elements. Now, the desired relative error is set equal to 1 per cent for each mode, and similar results are obtained. Figures 8 and 9 show the convergence curves and the effectivity indices, respectively, when all the modes are considered simultaneously in the analysis. The global refinement contribution factors obtained via the proposed method can be seen in Figure 10. The modes 9 and 10 have a significant weight in the mesh, and their contribution differs from that found in the case of linear elements. The other modes are shown to have a negligible effect.

The second test problem consists of a more complex domain (an expansion chamber), whose geometry is similar to that used in reference [14]. The fluid properties and the number of modes are kept equal to those of the previous example. First, four meshing steps and linear triangular elements are considered. The desired relative error is 5 per cent and the starting mesh is the same for all the modes. The mode shapes and the final meshes obtained by considering the modes separately are represented in Figure 11. The fourth, eighth, ninth and tenth modes produce very refined meshes to achieve the desired error. Figure 12 depicts the convergence of the estimated error for the meshes associated with modes 4 and 10, and

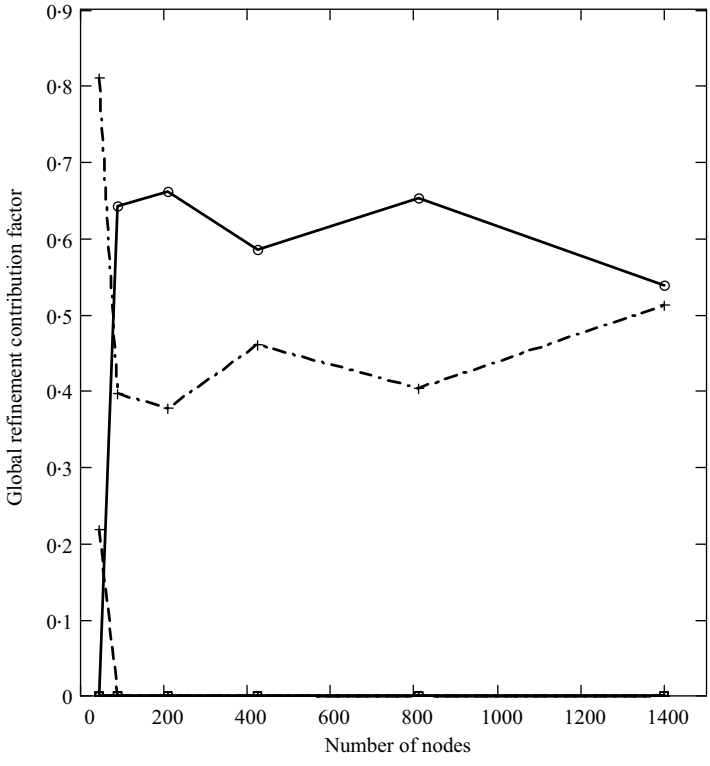

Figure 10. Global refinement contribution factors with quadratic triangular elements (legend same as in Figure 3).

again, the refinement is not suitable for some of the other modes, whose error is higher than the desired one. To save this drawback, all the modes can be considered at the same time, giving the meshes shown in Figure 13, which have been obtained by means of the present method and the minimum element size criterion (again the same starting mesh as in Figure 11 is considered, and it is depicted in Figure 13(a)). Both meshes are found to be quite similar, as it was justified in a previous section. The global refinement contribution factors of the modes 4, 8, 9 and 10 are found to be the most important in the *h*-adaptive process, as can be concluded from Figure 14 (it is worth noticing that the highest contribution factor corresponds to mode 4). The convergence of the relative error applying these two methods is represented in Figure 15. In both cases, the achieved error is less than or equal to the desired one for each mode. The former method provides the desired value for those modes that participate in the refinement, and a lower value for the rest. The latter gives similar results.

Regarding the use of quadratic elements, a desired error of 2 per cent and six steps are considered. Figure 16 shows the convergence of the estimated error for the two previous techniques. Now, the curves slightly differ, but the error is always lower than or equal to the required one. The participation factors are shown in Figure 17. Modes 4, 8 and 9 define the *h*-adaptive process, whereas mode 10 has been excluded (in the case of linear elements, this mode also takes part in the mesh refinement). Moreover, the influence of the fourth mode is higher in comparison with that associated with the three-noded element.

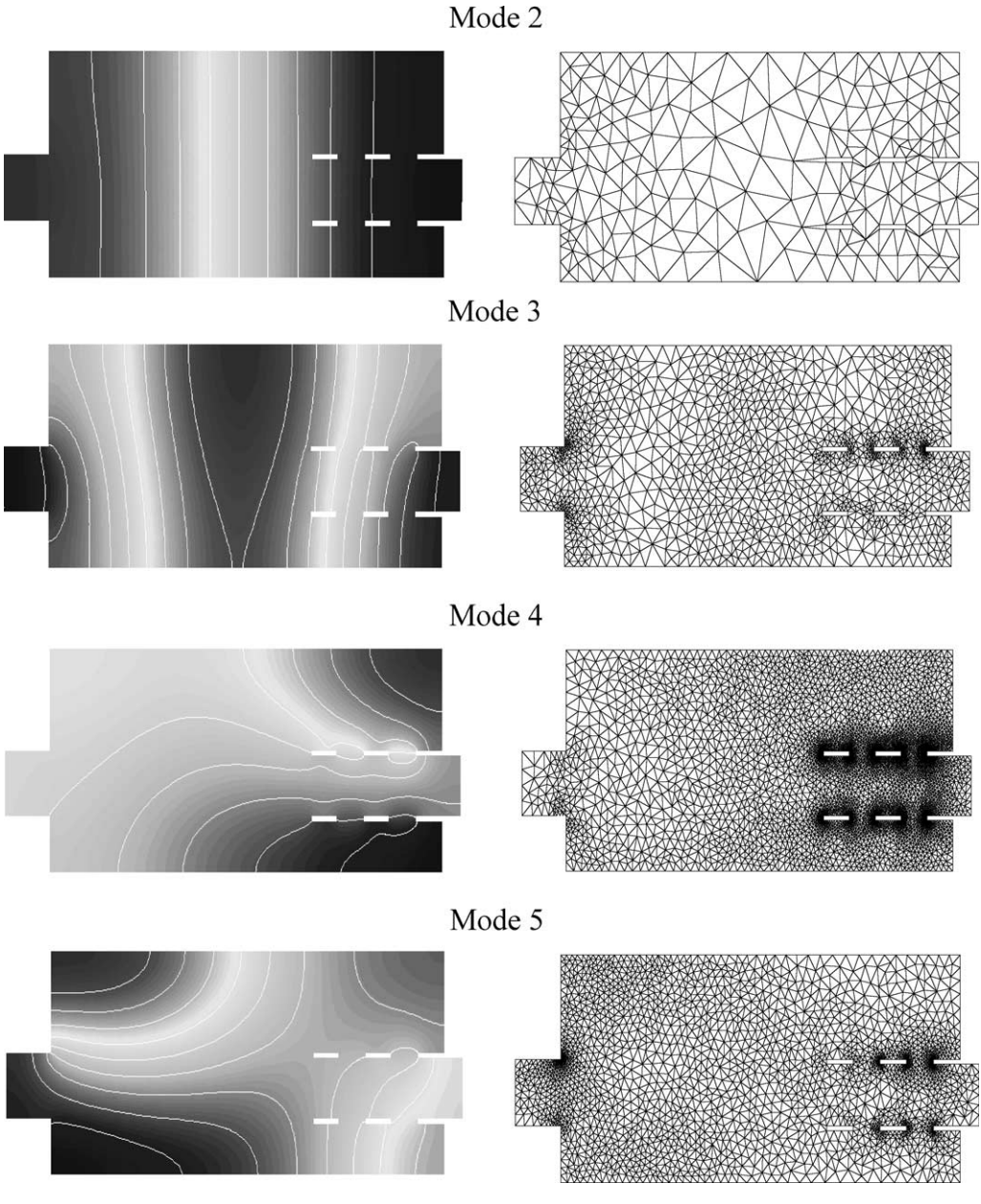

Figure 11. Acoustic mode shapes and optimum finite element meshes of an expansion chamber (modes considered separately).

6. CONCLUDING REMARKS

This work considers the error estimation in acoustic eigenproblems in which consistent mass matrices are used. The effectivity index achieved by means of the Zienkiewicz–Zhu estimator (extended by Bouillard *et al.* [4] to acoustic problems) is quite close to unity, thus

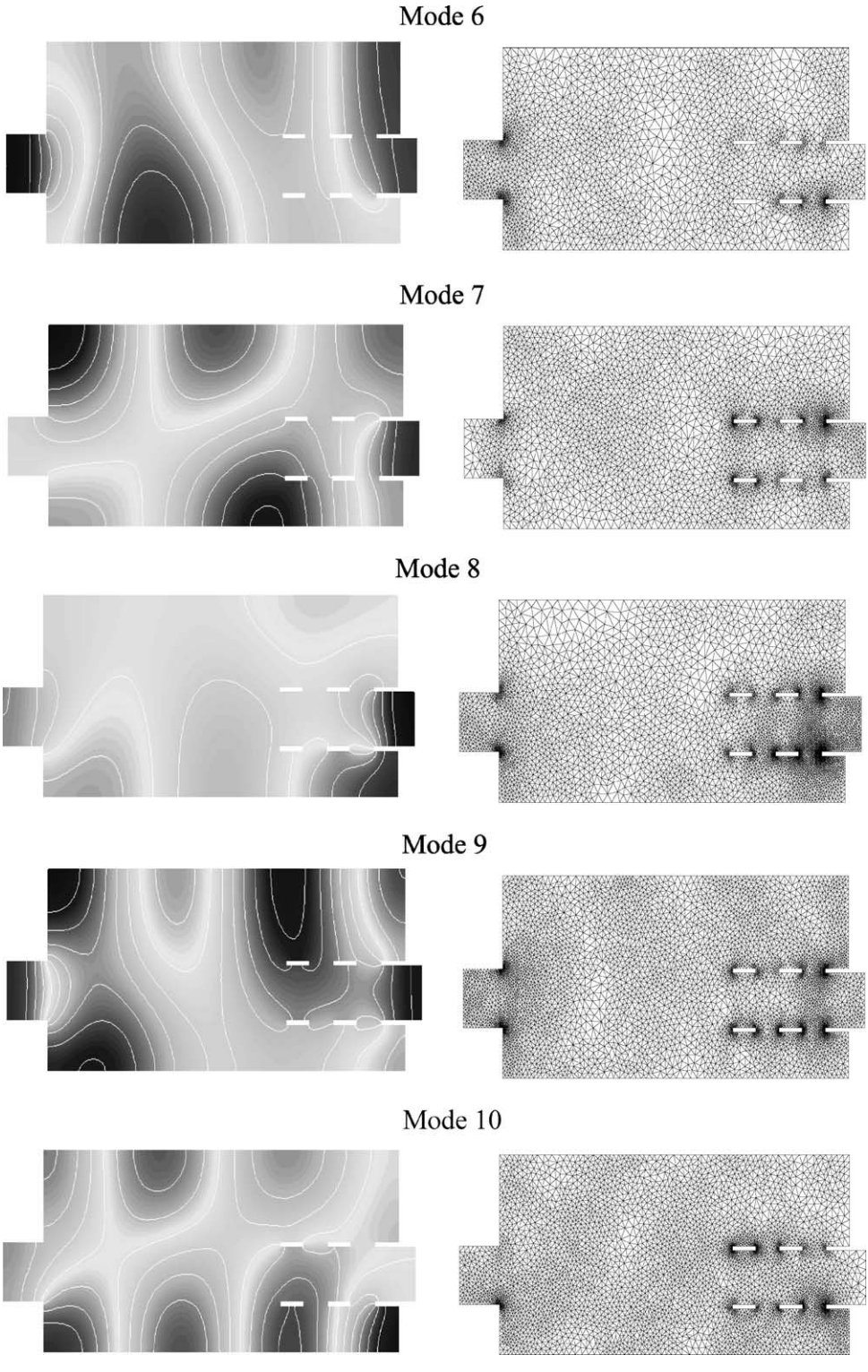

Figure. 11. Continued.

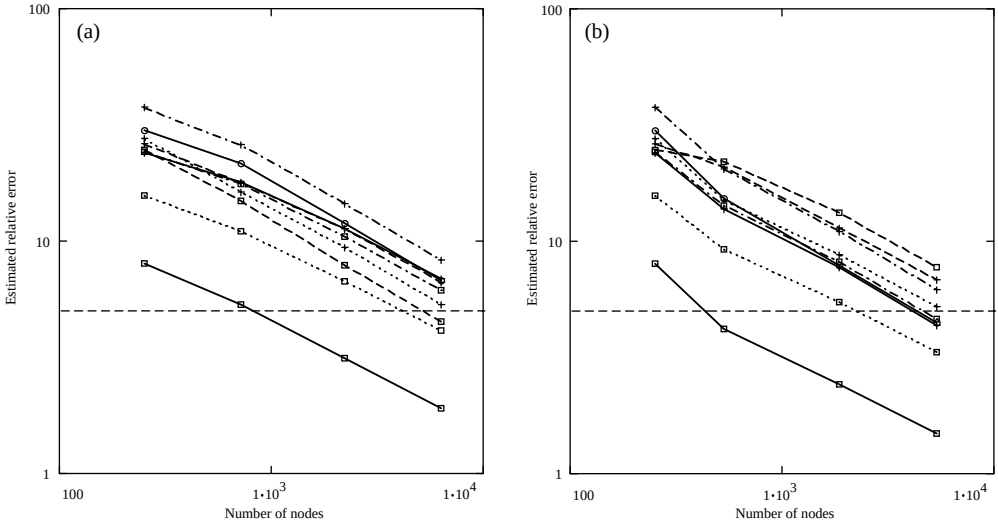

Figure 12. Convergence of the estimated relative error (legend same as in Figure 3). Mesh obtained considering only (a) mode 4 and (b) mode 10.

providing a reliable tool to perform the mesh refinement. A finite element refinement strategy has been proposed that allows the inclusion of a set of acoustic natural frequencies and mode shapes simultaneously in the analysis. This procedure gives a finite element mesh with a minimum number of elements, in which the estimated error is less than the required one for each natural frequency. The technique includes the influence of each mode shape, which is represented by means of its global refinement contribution factor. In addition, it has been justified that the traditional minimum element size criterion can be quite similar to the proposed technique.

ACKNOWLEDGMENT

The authors wish to thank the support received from Ministerio de Ciencia y Tecnología by means of the Project DPI2000-0743-C02-01.

REFERENCES

1. K. HONG and J. KIM 1995 *Journal of Sound and Vibration* **183**, 327–351. Natural mode analysis of hollow and annular elliptical cylindrical cavities.
2. A. SELAMET and Z. L. JI 2000 *Journal of Sound and Vibration* **229**, 3–19. Acoustic attenuation performance of circular expansion chambers with single-inlet and double-outlet.
3. P. L. GEORGE 1991 *Automatic Mesh Generation*. Chichester, U.K.: John Wiley and Sons.
4. P. BOUILLARD, J. F. ALLARD and G. WARZÉE 1996 *Communications in Numerical Methods in Engineering* **12**, 581–594. Superconvergent patch recovery technique for the finite element method in acoustics.
5. O. C. ZIENKIEWICZ and J. Z. ZHU 1992 *International Journal for Numerical Methods in Engineering* **33**, 1331–1364. The superconvergent patch recovery technique and *a posteriori* error estimates. Part 1: the recovery technique.

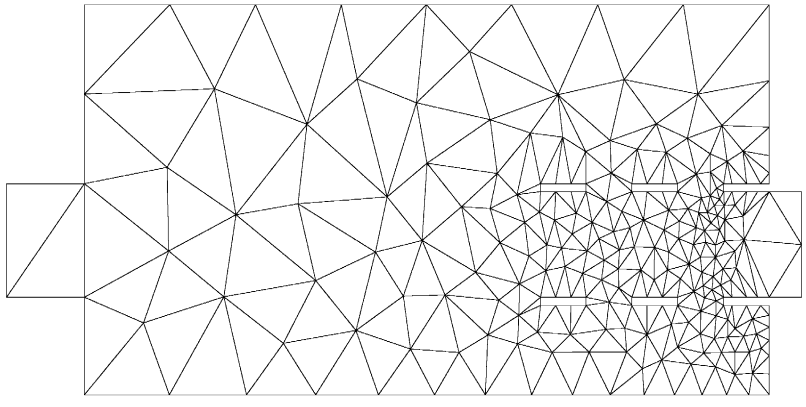

(a)

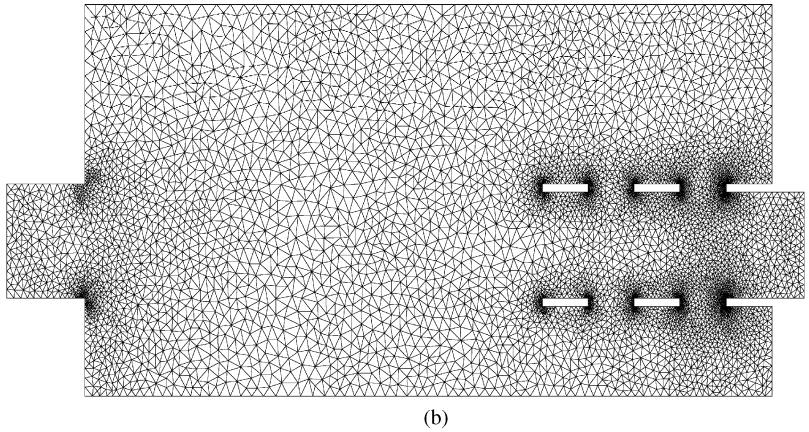

(b)

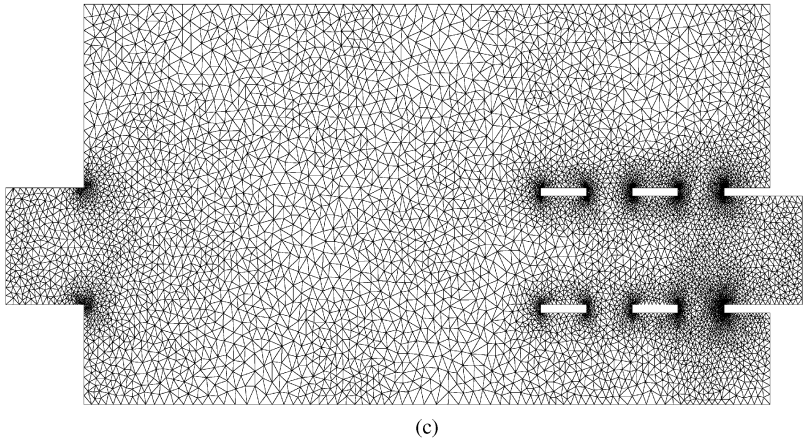

(c)

Figure 13. Finite element mesh for an expansion chamber with all the modes considered simultaneously: (a) starting mesh, (b) final mesh, minimum number of elements and (c) final mesh, minimum element size criterion.

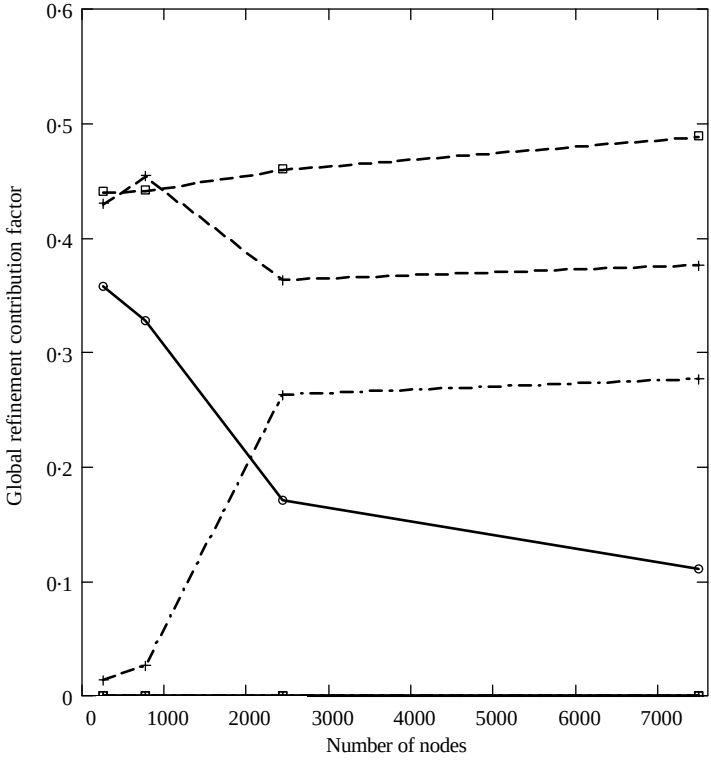

Figure 14. Global refinement contribution factors (legend same as in Figure 3).

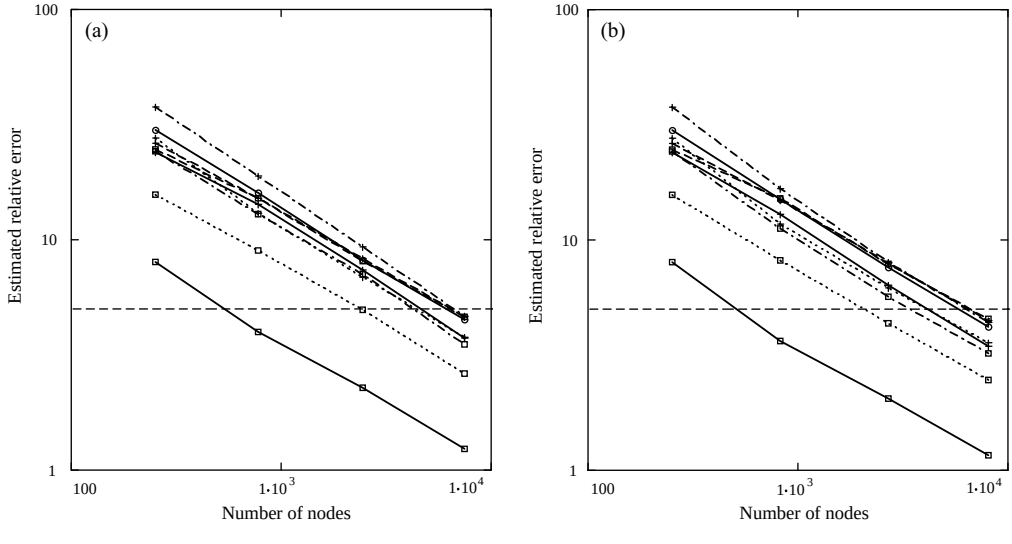

Figure 15. Convergence of the estimated relative error with the developed procedure and linear triangular elements (legend same as in Figure 3): (a) minimum number of elements and (b) minimum element size criterion.

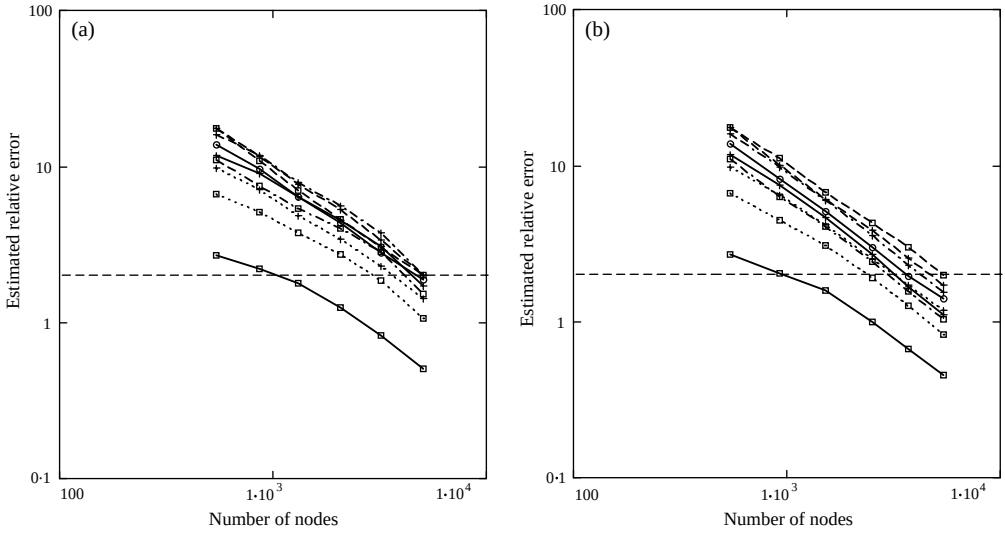

Figure 16. Convergence of the estimated relative error with the developed procedure and quadratic triangular elements (legend same as in Figure 3): (a) minimum number of elements and (b) minimum element size criterion.

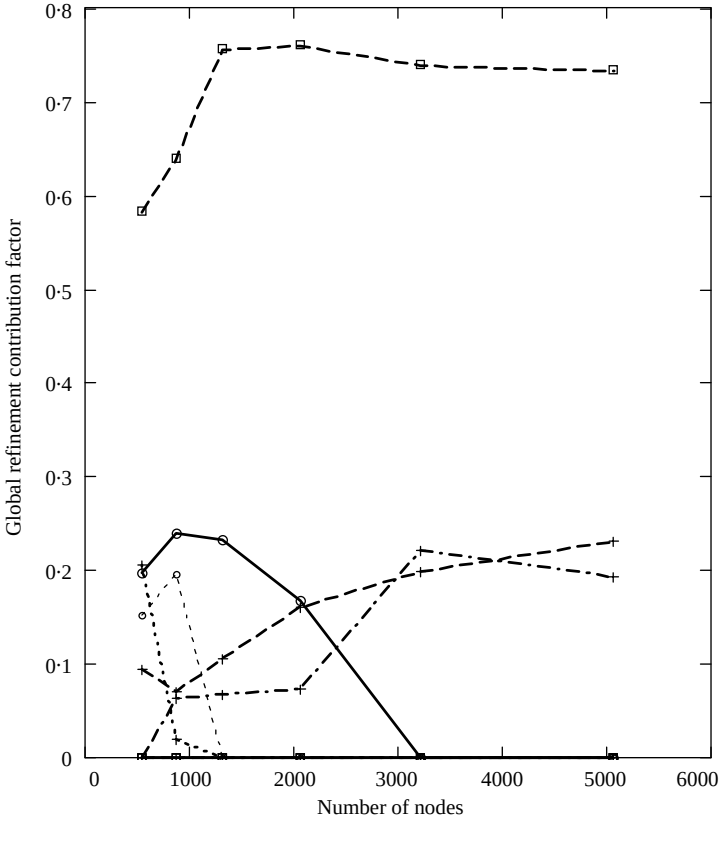

Figure 17. Global refinement contribution factors with quadratic triangular elements (legend same as in Figure 3).

6. O. C. ZIENKIEWICZ and J. Z. ZHU 1992 *International Journal for Numerical Methods in Engineering* **33**, 1365–1382. The superconvergent patch recovery technique and *a posteriori* error estimates. Part 2: error estimates and adaptivity.
7. F. IHLENBURG and I. BABUŠKA 1995 *Computational Mathematics and Applications* **30**, 9–37. Finite element solution of the Helmholtz equation with high wave number. Part I: the *h*-version of the FEM.
8. F. IHLENBURG and I. BABUŠKA 1997 *SIAM Journal on Numerical Analysis* **34**, 315–358. Finite element solution of the Helmholtz equation with high wave number. Part II: the *h*–*p* version of the FEM.
9. I. BABUŠKA, F. IHLENBURG, T. STROUBOULIS and S. K. GANGARAJ 1997 *International Journal for Numerical Methods in Engineering* **40**, 3443–3462. *A posteriori* error estimation for finite element solutions of Helmholtz' equation. Part I: the quality of local indicators and estimators.
10. J. L. RESTREPO 1997 *Ph.D. Thesis, Universidad Politécnica de Valencia*. H-adaptatividad de Elementos Finitos en Análisis de Frecuencias Naturales (in Spanish).
11. F. J. FUENMAYOR, J. L. RESTREPO, J. E. TARANCÓN and L. BAEZA 2001 *Finite Elements in Analysis and Design* **38**, 137–153. Error estimation and *h*-adaptive refinement in the analysis of natural frequencies.
12. D. B. STEPHEN and G. P. STEVEN 1997 *Journal of Sound and Vibration* **200**, 151–165. Natural frequency error estimation using a patch recovery technique.
13. P. HAGER and N. E. WIBERG 1999 *Computer Methods in Applied Mechanics and Engineering* **176**, 441–462. Adaptive eigenfrequency analysis by superconvergent patch recovery.
14. R. BAUŠYS and N. E. WIBERG 1999 *Journal of Sound and Vibration* **226**, 905–922. Adaptive finite element strategy for acoustic problems.
15. N. E. WIBERG and R. BAUŠYS 1999 IV *Congreso Métodos Numéricos en Ingeniería, Seville, Spain*. Error estimation and adaptivity for FE-analysis in acoustics.
16. P. LADEVEZE, G. COFFIGNAL and J. P. PELLE 1986 in *Accuracy Estimates and Adaptive Refinements in Finite Element Computations* (I. Babuška, O. C. Zienkiewicz, J. Gago and E. R. de A. Oliveira, editors), 181–203. London: Wiley-Interscience. Accuracy of elastoplastic and dynamic analysis.
17. P. LADEVEZE and J. P. PELLE 1989 *International Journal for Numerical Methods in Engineering* **28**, 1929–1949. Accuracy in finite element computation for eigenfrequencies.
18. M. L. MUNJAL 1987 *Acoustics of Ducts and Mufflers*. New York: Wiley-Interscience.
19. P. TONG, T. H. H. PIAN and L. L. BUCCIARELLI 1971 *Computers and Structures* **1**, 623–638. Mode shapes and frequencies by finite element method using consistent and lumped masses.
20. P. LADEVEZE and D. LEGUILLON 1983 *SIAM Journal on Numerical Analysis* **20**, 485–509. Error estimate procedure in the finite element method and applications.
21. P. LADEVEZE, P. MARIN and J. P. PELLE 1992 *Computer Methods in Applied Mechanics and Engineering* **94**, 303–315. Accuracy and optimal meshes in finite element computation for nearly incompressible materials.
22. P. COOREVITS, P. LADEVEZE and J. P. PELLE 1995 *Computer Methods in Applied Mechanics and Engineering* **121**, 91–120. An automatic procedure with control of accuracy for finite element analysis in 2D elasticity.
23. F. J. FUENMAYOR and J. L. OLIVER 1996 *International Journal for Numerical Methods in Engineering* **39**, 4039–4061. Criteria to achieve nearly optimal meshes in the *h*-adaptive finite element method.
24. L. Y. LI and P. BETTES 1996 *Communications in Numerical Methods in Engineering* **39**, 4039–4061. Notes on mesh optimal criteria in adaptive finite element computations.
25. F. J. FUENMAYOR, J. L. RESTREPO, J. J. RÓDENAS and J. E. TARANCÓN 1998 in *Proceedings of the Fourth World Congress on Computational Mechanics, Computational Mechanics, New Trends and Applications* (S. R. Idelsohn, E. Oñate and E. N. Dvorkin, editors), 181–203. A formulation of optimal mesh for problems with multiple analysis conditions.